PHILOSOPHICAL TRANSACTIONS OF THE ROYAL SOCIETY A
MATHEMATICAL, PHYSICAL & ENGINEERING SCIENCES

Imaging with Optically Generated Thermal Waves [and Discussion]

G. Busse, R. J. Dewhurst, M. Nikoonahad and C. B. Scruby

Phil. Trans. R. Soc. Lond. A 1986 **320**, 181-186
doi: 10.1098/rsta.1986.0109

Phil. Trans. R. Soc. Lond. A **320**, 181–186 (1986)
Printed in Great Britain

Imaging with optically generated thermal waves

By G. Busse†

Institut für Kunststoffprüfung und Kunststoffkunde, Universität Stuttgart, D-7000 Stuttgart 80, F.R.G.

By absorption of modulated optical power, a thermal wave is generated that interacts with thermal discontinuities. Imaging with scanned local thermal-wave probing is suited for non-contacting and non-destructive inspection of thermal structures in solids.

Introduction: 1. Thermal waves

Temperature propagation in a solid is described by a differential equation which is, for the one-dimensional case,

$$\partial^2 T/\partial z^2 = (\rho c/k)(\partial T/\partial t) \tag{1}$$

(Carslaw 1959), with temperature T, coordinate z, mass density ρ, specific heat c, thermal conductivity k, and time t.

This type of equation is known from diffusion. As the equation is not symmetrical with respect to time inversion, it describes an irreversible process which steadily reduces existing gradients. On this basis it is difficult to imagine what a thermal wave could be.

A wave is characterized by a periodicity in time and space. The question is, therefore, whether a temperature periodicity in time is correlated with a periodicity along the z-coordinate. If temperature is modulated at the plane $z = 0$ at the angular frequency ω and with amplitude ΔT_0, then the modulation at $z > 0$ is (Carslaw & Jaeger 1959)

$$\Delta T(z, t) = \Delta T_0 \exp(-z/\mu) \sin(\omega t - z/\mu). \tag{2}$$

The temperature modulation decreases exponentially with distance z, the phase lag $\psi = z/\mu$ between the modulation at $z = 0$ and $z > 0$ is proportional to the distance z travelled, as it is known for waves. The quantity μ ('thermal diffusion length'), given by

$$\mu = \surd(2k/\omega\rho c), \tag{3}$$

is typically of the order of millimetres for metals with a modulation frequency of 10 Hz. For polymers, μ is smaller by more than an order of magnitude. Wavelength is $2\pi\mu$. On this distance the amplitude decays to $\exp(-2\pi) \approx \frac{1}{500}$. The thermal wave generated by periodical heat diffusion, therefore, is a highly attenuated and slow scalar wave with a strong dispersion; phase velocity is proportional to the square root of modulation frequency, group velocity is twice the phase velocity (several centimetres per second for metals with a modulation frequency of 10 Hz). Non-sinusoidal waves would be distorted, that is the reason why most thermal wave experiments are done with modulated continuous wave (cw) sources and not with pulses.

For optical generation of thermal waves, one irradiates the absorbing sample surface with

† Permanent address: Institut für Physik, Universität der Bundeswehr München, D-8014 Neubiberg, F.R.G.

modulated laser light. Energy is deposited periodically, a temperature modulation is generated in a remote way. By focusing the laser beam to a small spot one obtains, to a good approximation, a point source from which a spherical thermal wave propagates into the sample.

2. Thermal wave transmission imaging

To detect a thermal wave any device that is sensitive to temperature modulation is suitable. Classical methods are 'opto (or photo)acoustic' detection based on thermal expansion (Bell 1881; Pao 1977; Rosencwaig 1980), recently developed 'photothermal' methods use the phase sensitive detection of modulated properties (Boccara *et al.* 1980; Ameri *et al.* 1981; Rosencwaig *et al.* 1983; Mundy *et al.* 1983) or of infrared emission (Nordal & Kanstad 1979). Some details are also given in review articles (Ash 1980). Although infrared detection is also used in thermography, one should keep in mind that photothermal infrared radiometry is an active method based on an induced temperature modulation thereby giving phase information. Photothermal infrared detection can therefore be considered as 'modulation thermography' or 'correlation thermography'.

An experimental arrangement for scanned thermal wave transmission imaging with this detection is shown in figure 1 (Busse 1980). The laser beam is modulated and focused to the opaque sample, which can be moved in a raster-like way with respect to the optical components, while at the rear surface the infrared detector monitors the temperature modulation. Spatially resolved information is obtained since both the thermal wave source and the detector are localized, therefore essentially a narrow thermal wave 'ray' (Burt 1981; Burt 1983) of the spherical thermal wave is monitored after it has travelled through the sample. From the locally observed phase lag one can determine either sample thickness or local thermal

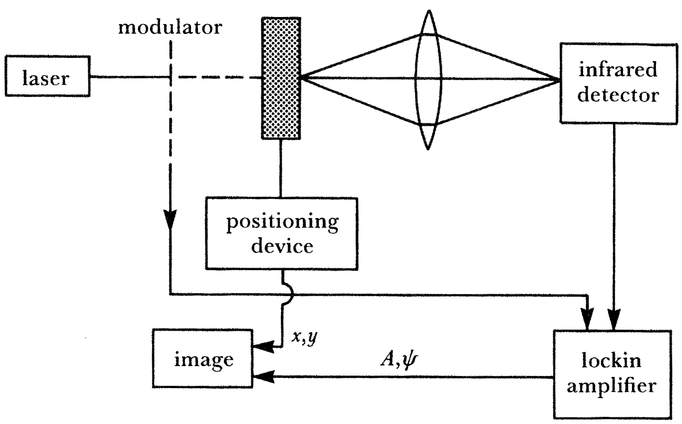

Figure 1. Experimental arrangement for thermal wave transmission imaging.

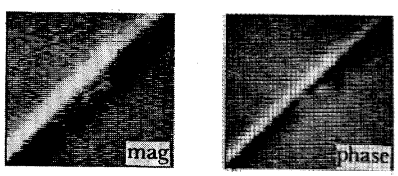

Figure 2. Thermal wave transmission image (magnitude and phase) of a seam in 0.1 mm stainless steel.

diffusion length, μ, averaged along the thermal wave ray. Thermal discontinuities affect this value, thereby allowing for their noncontacting detection.

A potential field of applications is seam inspection, shown in figure 2. Both signal magnitude and phase can be used for imaging. However, phase images are true thermal wave images, while magnitude images are contrasted with optical surface structures (Rosencwaig & Busse 1980) and, in the case of photothermal infrared detection, by structures of the infrared emission coefficient. Other methods of detection correspondingly display structures of the physical properties involved.

Another field of applications is polymer inspection: coating thickness, delamination, curing, fibre content and orientation have been investigated (Busse & Eyerer 1983; Almond *et al.* 1985).

Although resolution may be better than with other arrangements, thermal wave transmission reveals only the projection of thermal structures, similar to X-ray images. However, this difficulty has been overcome with stereoscopic detection where depth information is obtained (Busse & Renk 1983). The basic disadvantages are the requirement of an access to both sides of the sample (inspection of hollow samples is not possible) and the inability to investigate near-surface regions of samples which are too thick for thermal wave transmission.

3. Thermal wave reflection imaging

Although less straightforward, this arrangement has been used first. The idea is that a thermal wave undergoes reflection at discontinuities. A subsurface flaw therefore modifies the thermal wave at the front surface of the sample by a superposed thermal wave coming back from internal boundaries. Signal change depends on how far the reflected wave has travelled. Theoretical and experimental investigations have been performed to determine this correlation (Rosencwaig & Gersho 1976; Busse 1979; Thomas *et al.* 1980; Bennett & Patty 1982; Lehto *et al.* 1981). The essential result is that, due to the addition of vectors in the complex signal plane, depth range is about thermal diffusion length, μ, for magnitude and about twice this if phase is used. As thermal diffusion length depends on modulation frequency, depth range can be varied. From the frequency dependent appearance of structures, three-dimensional information is obtained (Busse & Rosencwaig 1980). As an example, figure 3 shows magnitude images of two subsurface holes ending in different depths beneath the surface in aluminium. The one in a larger depth disappears at higher modulation frequencies.

As both the thermal wave source and the detector are on the same side of the sample, inspection of near-surface regions of thick samples is possible whereas the transmitted thermal

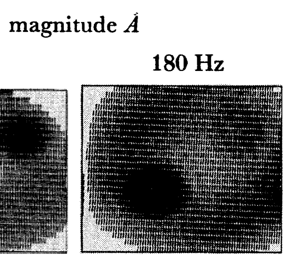

FIGURE 3. Magnitude imaging of an aluminium sample with two holes ending 0.2 mm (left hole) and 0.4 mm below the surface (Busse & Rosencwaig 1980).

wave would be too weak to be detected. This makes the front-surface arrangement attractive for applications with the various methods (Wong *et al.* 1979; Boccara *et al.* 1980; Aamodt *et al.* 1981; Jackson *et al.* 1981; Thomas *et al.* 1982; Rosencwaig *et al.* 1983).

One application of permanent interest is crack detection. Here the result depends on the detector geometry involved. Detection with a microphone gives a signal that is proportional to the surface integral of the thermal wave, whereas photothermal beam deflection depends on a line integral. A closed crack perpendicular to the surface cannot be found in the first case, whereas this is possible in the second case (Grice *et al.* 1983).

Another field of interest is the inspection of integrated circuits (Rosencwaig & Busse 1980) since thermal features can be imaged which are beneath the optical surface, as is shown in figure 4 where the magnitude image is dominated by optical features, while the phase angle image shows the thermal structure of the same region. This experiment has been performed with piezoelectric detection at 200 KHz. These high frequencies are needed for thermal-wave microscopy (Rosencwaig 1979).

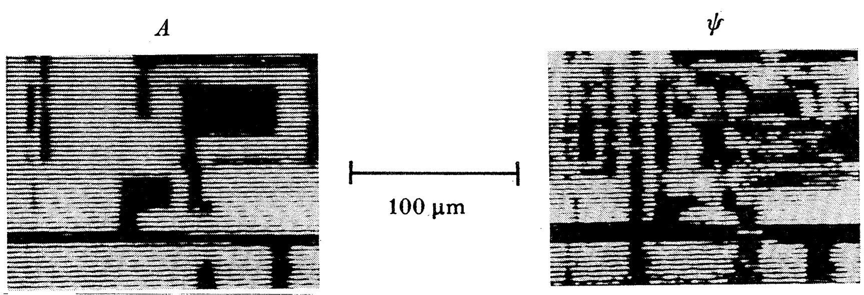

FIGURE 4. Magnitude (*A*) and phase image (*ψ*) of an integrated circuit at 200 kHz.

Front-surface seam inspection is of technical interest as it is more convenient, however, the information obtained may be less significant than with the transmission arrangement (Busse 1982). As an example, figure 5 shows a seam in stainless steel with rear-surface (a) and front-surface detection (b). The information on the defect is more significant with phase-angle transmission imaging.

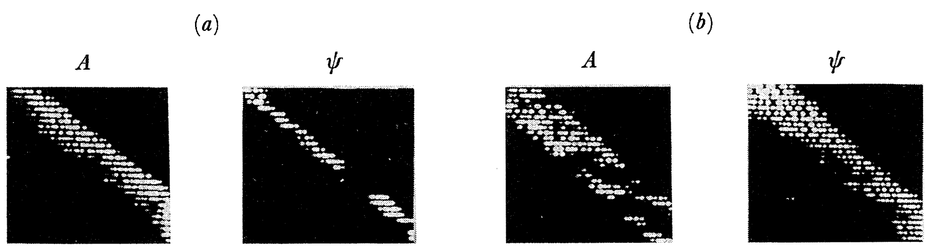

FIGURE 5. Comparison of results obtained with thermal wave transmission (*a*) and reflection (*b*) both with signal magnitude and phase *ψ*. Field of view is 2.3 mm × 2.3 mm^2.

4. Conclusion

Imaging with optically generated thermal waves reveals thermal structures although no physical contact with the sample is required. The information differs from that obtained with other methods of non-destructive testing. From what has been found till now it seems that only near-surface regions can be inspected (millimetre-region in metals, a tenth of that in polymers). This method, therefore, is not intended to compete with existing methods, but it may give additional information that cannot be obtained otherwise.

References

Aamodt, L. C. & Murphy, J. C. 1981 Photothermal measurement using a localized excitation source. *J. appl. Phys.* **52**, 4903–4914.
Almond, D. P., Patel, P. M., Pickup, I. M. & Reiter, H. 1985 An evaluation of the suitability of thermal wave interferometry for the testing of plasma sprayed coatings. *NDT Int.* **18**, 17–24.
Ameri, S., Ash, E. A., Neuman, V. & Petts, C. R. 1981 Photodisplacement imaging. *Electron. Lett.* **17**, 337–338.
Ash, E. A. 1980 *Scanned image microscopy*. London: Academic Press.
Bell, A. G. 1881 Upon the production of sound by radiant energy. *Phil. Mag.* **11**, 510–528.
Bennett, C. A. & Patty, R. R. 1982 Thermal wave interferometry: a potential application of the photoacoustic effect. *Appl. Opt.* **21**, 49–54.
Boccara, A. C., Fournier, D. & Badoz, J. 1980 Thermo-optical spectroscopy: detection by the 'mirage effect'. *Appl. Phys. Lett.* **36**, 130–132.
Burt, J. A. 1981 Thermal wave diffraction imaging. In *Proc. IEEE Ultrasonics Symp.* pp. 815–816.
Burt, J. A. 1983 Ray theory of thermal wave imaging. *J. Physique, Paris, Coll.* **C6**, 453–457.
Busse, G. 1979 Optoacoustic phase angle measurement for probing a metal. *Appl. Phys. Lett.* **35** 759–760.
Busse, G. 1980 Photothermal transmission probing of a metal. *Infrared Phys.* **20**, 419–422.
Busse, G. 1982 Optoacoustic and photothermal material inspection techniques. *Appl. Opt.* **21**, 107–110.
Busse, G. & Eyerer, P. 1983 Thermal wave remote and non-destructive inspection of polymers. *Appl. Phys. Lett.* **43**, 355–358.
Busse, G. & Renk, K. F. 1983 Stereoscopic depth analysis by thermal wave transmission for nondestructive evaluation. *Appl. Phys. Lett.* **42**, 366–368.
Busse, G. & Rosencwaig, A. 1980 Subsurface imaging with photoacoustics. *Appl. Phys. Lett.* **36**, 815–816
Carslaw, H. S. 1959 *Conduction of heat in solids*. 2nd edn. Oxford: Clarendon Press.
Grice, K. R., Inglehart, L. J., Favro, L., Kuo, P. K. & Thomas, R. L. 1983 Thermal wave imaging of closed cracks in solids. *J. appl. Phys.* **54**, 6245–6255.
Jackson, W. B., Amer, N. M., Boccara, A. C. & Fournier, D. 1981 Photothermal deflection spectroscopy and detection. *Appl. Opt.* **20**, 1333–1344.
Lehto, A., Jaarinen, J., Tiusanen, T., Jokinen, M. & Luukala, M. 1981 Magnitude and phase in thermal wave imaging. *Electron. Lett.* **17**, 364–365.
Mundy, W. C., Hughes, R. S. & Carniglia, C. K. 1983 Photothermal deflection microscopy of dielectric thin films. *Phys. Lett.* **39**, 985–987.
Nordal, P.-E. & Kanstad, S. O. 1979 Photothermal radiometry. *Physica Scr.* **20**, 659–662.
Pao, Y.-H. 1977 *Optoacoustic spectroscopy and detection*. New York: Academic Press.
Rosencwaig, A. 1979 Photoacoustic microscopy. *Am. Lab.* **11**, pp. 39–49.
Rosencwaig, A. 1980 *Photoacoustics and photoacoustic spectroscopy*. New York: John Wiley and Sons.
Rosencwaig, A. & Busse, G. 1980 High-resolution photo-acoustic thermal-wave microscopy. *Appl. Phys. Lett.* **36**, 725–727.
Rosencwaig, A. & Gersho, A. 1976 Theory of the photoacoustic effect with solids. *J. appl. Phys.* **47**, 64–69.
Rosencwaig, A., Opsal, J. & Willenborg, D. L. 1983 Thin film thickness measurements with thermal waves. *Appl. Phys. Lett.* **43**, 166–168.
Thomas, R. L., Pouch, J. J., Wong, Y. H., Favro, L. D., Kuo, P. K. & Rosencwaig, A. 1980 Subsurface flaw detection in metals by photoacoustic microscopy. *Appl. Phys.* **51**, 1152–1156.
Thomas, R. L., Favro, L. D., Grice, K. R., Inglehart, L. J., Kuo, P. K., Lhota, J. & Busse, G. 1982 In *Proc. IEEE Ultrasonics Symp.*, pp. 586–590.
Wong, Y. H., Thomas, R. L. & Pouch, J. J. 1978 Surface and subsurface structure of solids by laser photoacoustic spectroscopy. *Appl. Phys. Lett.* **32**, 538–539.

Discussion

R. J. Dewhurst (*Department of Applied Physics, University of Hull, U.K.*). Dr Busse has discussed imaging techniques which have mainly used an infrared detector. However, he also mentioned the possibility of photoacoustic detection. What advantages, if any, do photoacoustic techniques offer?

G. Busse. Photoacoustic detection with the use of a microphone cell or piezoelectric material is an integrating process; the whole thermal wave is observed. This is an advantage for the signal:noise ratio, it also eliminates the need of a sophisticated detector alignment. Besides ease of use one should mention, as another advantage, that these detectors are inexpensive.

The basic disadvantage, however, is the need of some physical contact with the sample and the inability to obtain spatially resolved thermal-wave detection.

M. Nikoonahad (*Philips Laboratories*, 345 *Scarborough Road, Briarcliff Manor, New York* 10510, *U.S.A.*). Has Dr Busse probed the temperature distribution at the back of a carbon fibre composite slab?

G. Busse. Yes, the distribution is not symmetrical.

M. Nikoonahad. What I really want to know is whether Dr Busse has observed beam-steering effects due to anisotropy of these materials.

G. Busse. There is some experimental indication of this.

M. Nikoonahad. When I was still at University College we did some theory on this which predicts beam-steering effects as well as beam distortion and it would be interesting to see whether Dr Busse observed such things in experiments.

G. Busse. I should be happy to compare our results with Dr Nikoonahad's theoretical predictions.

C. B. Scruby (*AERE Harwell, Oxfordshire, U.K.*). How long does it take to produce a scanned image, and is this a drawback for practical applications of the technique?

G. Busse. The time taken to produce a scanned image depends on the number of image elements ('pixels') and the required signal:noise ratio (determining the time per pixel). The time therefore ranges from 1 min to about 1 h. This is a drawback for applications, but the information cannot be obtained otherwise. If other techniques provide enough information in a shorter time, maybe they should be preferred.

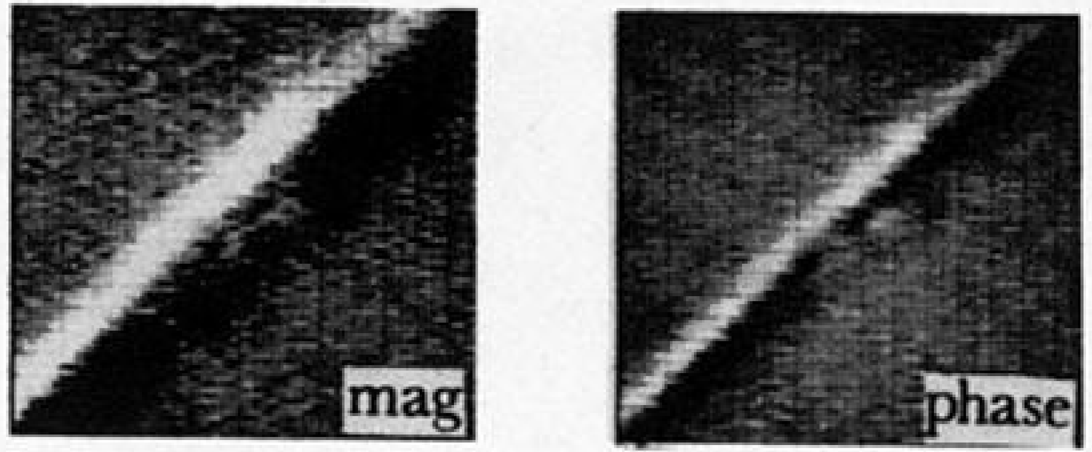

FIGURE 2. Thermal wave transmission image (magnitude and phase) of a seam in 0.1 mm stainless steel.

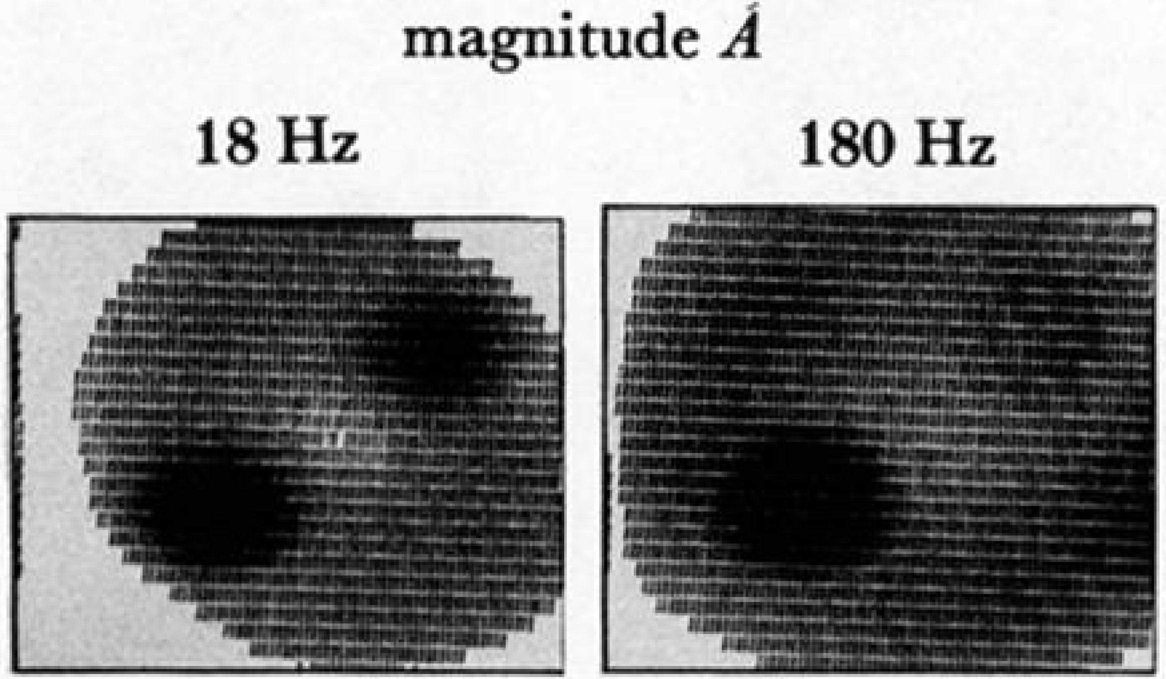

FIGURE 3. Magnitude imaging of an aluminium sample with two holes ending 0.2 mm (left hole) and 0.4 mm below the surface (Busse & Rosencwaig 1980).

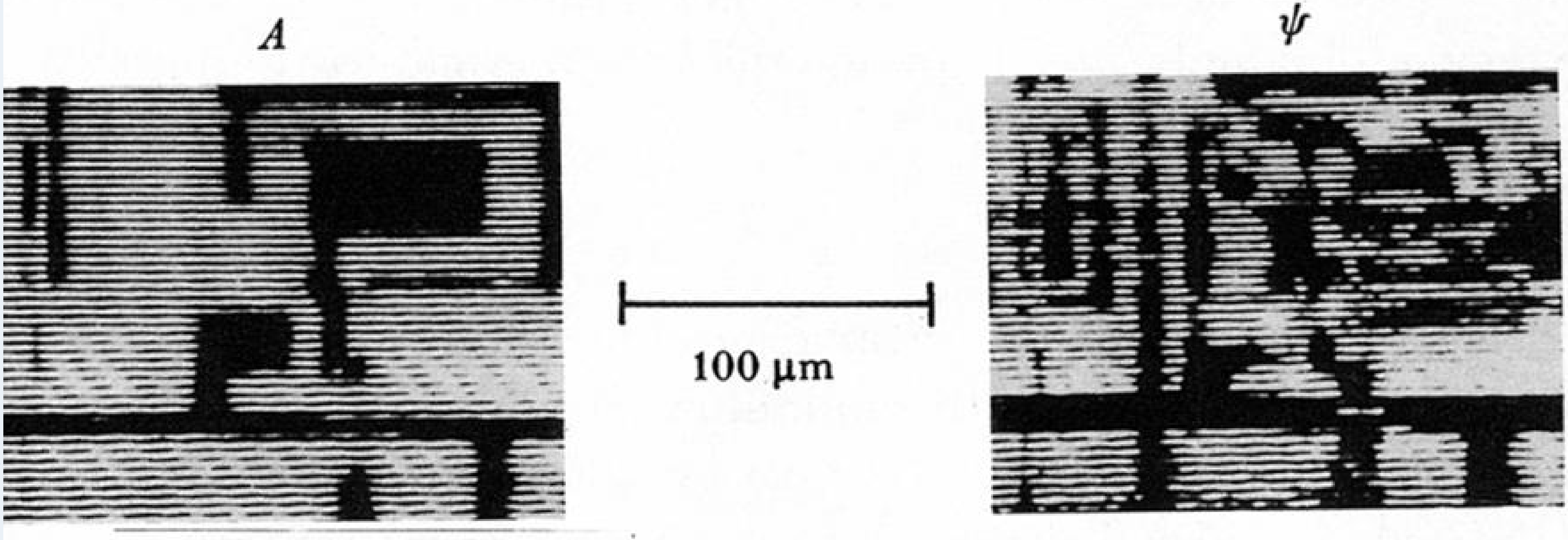

FIGURE 4. Magnitude (A) and phase image (ψ) of an integrated circuit at 200 kHz.

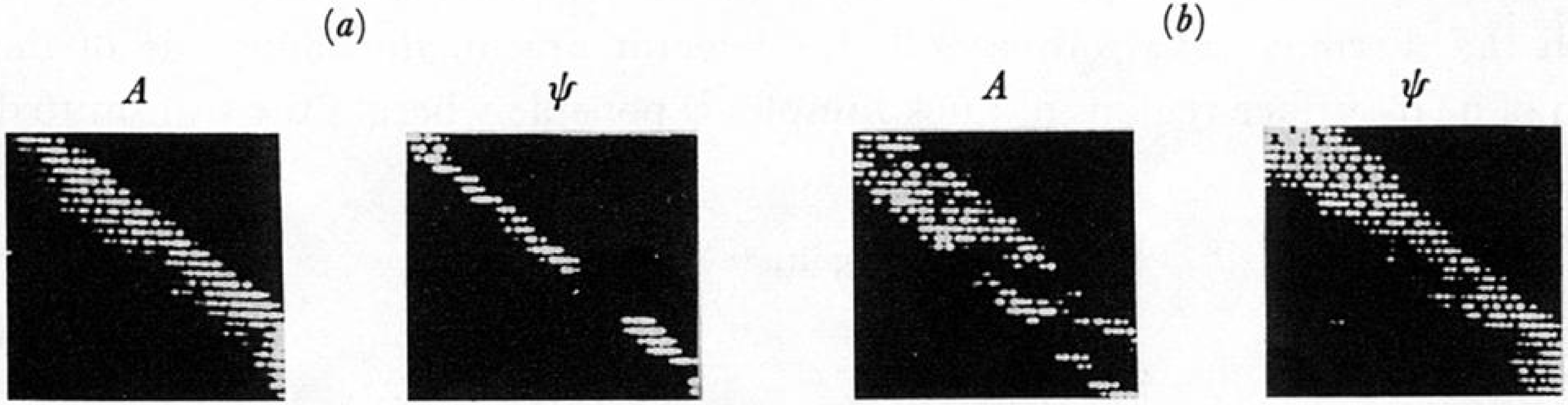

IGURE 5. Comparison of results obtained with thermal wave transmission (*a*) and reflection (*b*) both with signal magnitude and phase ψ. Field of view is 2.3 mm × 2.3 mm².